Bending reorientational solitons with modulated alignment

Bending reorientational solitons with modulated alignment

FILIP A. SALA[1], NOEL F. SMYTH[2], URSZULA A. LAUDYN[1], MIROSŁAW A. KARPIERZ[1], ANTONMARIA A. MINZONI[3], AND GAETANO ASSANTO[4,5,*]

[1] Warsaw University of Technology, Faculty of Physics, Warsaw 00-662, Poland
[2] School of Mathematics, University of Edinburgh, Edinburgh EH9 3FD, Scotland, U.K.
[3] Universidad Nacional Autónoma de México, Department of Mathematics and Mechanics, Instituto de Investigación en Matemáticas Aplicádas y Sistemas, México D.F. 01000, México
[4] University of Rome "Roma Tre", NooEL– Nonlinear Optics and OptoElectronics Lab, Rome 00146, Italy
[5] Tampere University of Technology, Photonics Laboratory, Tampere FI-33101, Finland
[*] Corresponding author: assanto@uniroma3.it

Compiled October 6, 2017

While curved waveguides are fundamental elements in photonics, those induced all-optically in nonlinear uniform dielectrics tend to be straight. In uniaxial soft matter with a reorientational response, such as nematic liquid crystals, light beams in the extraordinary polarization undergo self-focusing via an increase in refractive index and eventually form spatial solitons, i.e., self-induced waveguides. Hereby we investigate the bending of such waveguides by analyzing the trajectory of solitons in nematic liquid crystals— nematicons— in the presence of a linearly varying transverse orientation of the optic axis. To this extent we use and compare two approaches: i) a slowly varying (adiabatic) approximation based on momentum conservation of the nematicon in a Hamiltonian sense; ii) the Frank-Oseen elastic theory coupled with a fully vectorial and nonlinear beam propagation method. The models provide comparable results in such a non-homogeneously oriented uniaxial medium and predict bent soliton paths with either monotonic or non-monotonic curvatures, enabling the design of curved channel waveguides induced by light beams.

OCIS codes: *(190.6135) Spatial solitons; (230.3720) Liquid-crystal devices; (160.3710) Liquid crystals; (190.3270) Kerr effect*

This paper is dedicated to one of its coauthors, Professor Antonmaria (Tim) A. Minzoni, who prematurely passed away during its preparation. N.F.S. and G.A. remember Tim as a generous person of vast culture, a dear friend and an outstanding colleague.

INTRODUCTION

All-optical or light-induced waveguides through the self-focusing response of optical materials are commonly referred to as spatial optical solitons and have been studied in several media [1], including liquid crystals [2]. Nematic liquid crystals (NLCs) are anisotropic, typically uniaxial, soft matter consisting of thread-like molecules which exhibit orientational but no spatial order [3]. The anisotropic molecules are in a fluid state, linked by elastic forces, and exhibit two refractive index eigenvalues, ordinary and extraordinary, for light polarized perpendicular or parallel to the optic axis, termed the molecular director and usually denoted by the unit vector $\vec{n}$. The refractive index of extraordinary polarized light has a nonlinear optical dependence through the reorientational response: the electric field of the light beam induces dipoles in the NLC molecules, so that they tend to rotate towards the field vector to minimize the system energy until the elastic response balances this electromechanical torque [3]. The resulting change in molecular orientation then changes the extraordinary refractive index towards the largest eigenvalue, so that the beam undergoes self-focusing. When the latter compensates linear diffraction, a $(2+1)D$ solitary wave can form, often termed a nematicon [2, 4]. Nematicons are non-diffracting solitary beams in nematic liquid crystals, confined by their own graded-index waveguides. They have been extensively investigated over a number of

years in many different scenarios, including planar cells [5–10], capillaries [11, 12], one-dimensional waveguides [13], coupled waveguides [4] and bulk [14]. When the wavevector of the light beam and the molecular director are neither perpendicular nor parallel, the Poynting vector of the nematicon walks-off the wavevector at a finite angle owing to the tensorial nature of the dielectric susceptibility [15]. Such an angular deviation of the energy flux depends on the refractive index eigenvalues, $n_{\parallel}$ and $n_{\perp}$ for electric fields parallel and perpendicular to the director, respectively, and the angle ψ between the director and wavevector. Nematicon walk-off can be exploited in optical devices, for instance, signal demultiplexers or routers [2, 16–19].

Similarly to other nonlinear optical media [1], in uniform NLCs nematicons propagate in rectilinear trajectories along their Pointing vector. The graded index waveguides associated with these spatial solitons are therefore straight. Curved nematicons have been investigated by introducing extra elements, such as graded interfaces [17, 18, 20], localized refractive index perturbations [2, 16, 21], interactions with boundaries [8, 22] as well as other solitons [2, 5, 9, 23, 24]. A detailed approach to designing and modeling beam-induced waveguides undergoing bending versus propagation in a medium without external perturbations, however, has never been developed before.

In this article we introduce and study -for the first time to the best of our knowledge- curved solitons as they propagate in nematic liquid crystals subject to a linearly varying orientation of the optic axis across one of the transverse coordinates, in the principal plane defined by optic axis and wavevector. We consider nematicons excited in a planar cell of fixed (uniform) thickness, with upper and lower interfaces treated to ensure planar anchoring of the NLC molecules. This geometry is radically different from those entailing spin-orbit interactions of light with matter [25, 26], as the optic axis and the wavevector are not mutually orthogonal because the light beam is an extraordinary wave . As the molecular alignment varies across the sample, both the extraordinary refractive index and the birefringent walk-off vary as well. These two variations determine the resulting trajectory of extraordinarily polarized beams in the cell, including the path of self-confined nematicons. To investigate non-rectilinear nematicon paths in a transversely modulated uniaxial we use two different approaches in the weakly nonlinear regime (i.e. power independent walk-off): (i) numerical solutions of the full governing Maxwell's equations employing a fully vectorial beam propagation method for the beam and the Frank-Oseen elastic theory for the NLC response [2]; (ii) an adiabatic (slowly varying) approximation to yield simplified forms of these equations, invoking momentum conservation [2, 27, 28]. The adiabatic approximation is based on the high nonlocality of the NLCs, which implies that the nonlinear response extends far beyond the transverse size of the optical wavepacket [2, 29] and decouples the amplitude/width evolution of the beam from its trajectory [28]. In this study the background director angle is slowly varying, typically 0.002 rad/μm in a cell of width 200 μm, so that the nematicon trajectory can be determined by "momentum conservation", in the sense of invariances of the Lagrangian for the NLC equations. The latter approach yields simple equations which have an exact solution and provides excellent agreement with the full numerical solutions, proving more than adequate to model beam evolution in non-uniform birefringent media.

GEOMETRY AND GOVERNING EQUATIONS

We consider the propagation of a linearly polarized, coherent light beam in a planar cell with undoped, positive uniaxial, nematic liquid crystals. The extraordinary polarized beam is taken to initially propagate forward in the z direction, with electric field E oscillating in the y transverse direction and x completing the coordinate triad. To eliminate the Freédericksz threshold [3] and maximize the nonlinear optical response [2], the cell interfaces perpendicular to x are rubbed so that the molecular director makes an angle θ_0 with z in the (y,z) plane everywhere in the bulk owing to elastic interactions, as sketched in Fig. 1. An additional y-dependent rotation $\theta_b(y)$ is given to the nematic director to modulate the uniaxial medium, as illustrated in Fig. 2(b). Due to the nonlinearity, the light beam can rotate the optic axis by an extra angle θ, so that the director forms a total angle $\psi(y) = \theta_0 + \theta_b(y) + \theta(y)$ to the z axis in the (y,z) plane [2].

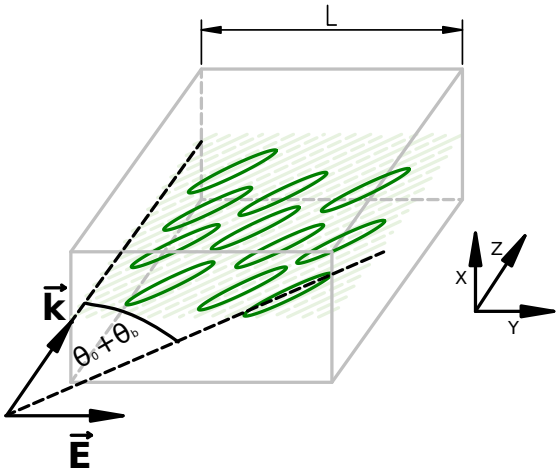

Fig. 1. (Color online) Sketch of the configuration and NLC alignment. The input Gaussian beam is linearly polarized along y.

Beam propagation method and elastic theory

One of the approaches used to study the nonlinear evolution of a light beam in nematic liquid crystals is the fully vectorial beam propagation method (FVBPM) [30] in conjunction with elastic theory based on the Frank-Oseen

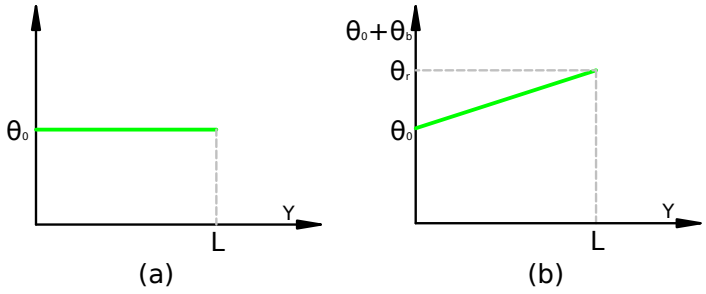

Fig. 2. (Color online) (a) Uniform and (b) linearly modulated anchoring conditions across y.

model for the NLC response [3, 31, 32]. The FVBPM can be derived directly from Maxwell's equations [33, 34], considering harmonically oscillating electric and magnetic fields in an anisotropic dielectric

$$\begin{aligned}
\frac{\partial H_z}{\partial y} - \frac{\partial H_y}{\partial z} &= i\omega\varepsilon_0\left(\varepsilon_{11}E_x + \varepsilon_{12}E_y + \varepsilon_{13}E_z\right), \\
\frac{\partial H_x}{\partial z} - \frac{\partial H_z}{\partial x} &= i\omega\varepsilon_0\left(\varepsilon_{21}E_x + \varepsilon_{22}E_y + \varepsilon_{23}E_z\right), \\
\frac{\partial H_y}{\partial x} - \frac{\partial H_x}{\partial y} &= i\omega\varepsilon_0\left(\varepsilon_{31}E_x + \varepsilon_{32}E_y + \varepsilon_{33}E_z\right), \\
H_x &= -\frac{1}{i\mu_0\omega}\left(\frac{\partial E_z}{\partial y} - \frac{\partial E_y}{\partial z}\right), \\
H_y &= -\frac{1}{i\mu_0\omega}\left(\frac{\partial E_x}{\partial z} - \frac{\partial E_z}{\partial x}\right), \\
H_z &= -\frac{1}{i\mu_0\omega}\left(\frac{\partial E_y}{\partial x} - \frac{\partial E_x}{\partial y}\right).
\end{aligned} \tag{1}$$

Here the complex amplitudes $\vec{E}$ and $\vec{H}$ are the electric and magnetic fields, respectively, ε is the electric permittivity tensor, ω is the angular frequency and μ_0 is the vacuum permeability. These coupled partial differential equations can be solved numerically, as the x and y derivatives can be approximated using standard central differences and the solution can be propagated forward along z using a standard fourth-order Runge-Kutta scheme. In this work the step size is chosen to be $dz = 10\,\text{nm}$. At the cell boundaries, reflective Dirichlet boundary conditions are imposed, so that $\mathbf{E} = 0$ and $\mathbf{H} = 0$ at the NLC/glass interfaces. The electric tensor in equations (1) is

$$\varepsilon = \begin{bmatrix} \varepsilon_\perp & 0 & 0 \\ 0 & \varepsilon_\perp + \Delta\varepsilon \sin^2\psi & \Delta\varepsilon \sin\psi\cos\psi \\ 0 & \Delta\varepsilon \sin\psi\cos\psi & \varepsilon_\perp + \Delta\varepsilon\cos^2\psi \end{bmatrix}, \tag{2}$$

with $\Delta\varepsilon = n_\parallel^2 - n_\perp^2$ the optical anisotropy. These electromagnetic equations are coupled to the NLC response, given by the Frank-Oseen expression for the energy density in the non-chiral case [3, 31, 32]

$$\begin{aligned}
f &= \frac{1}{2}K_{11}(\nabla\vec{n})^2 + \frac{1}{2}K_{22}(\vec{n}\cdot(\nabla\times\vec{n}))^2 \\
&\quad + \frac{1}{2}K_{33}(\vec{n}\times(\nabla\times\vec{n}))^2 - \frac{1}{2}\varepsilon_0\Delta\varepsilon(\vec{n}\cdot\vec{E})^2.
\end{aligned} \tag{3}$$

Here, K_{11}, K_{22}, K_{33} are the Frank elastic constants for bend, twist and splay deformations of the molecular director $\vec{n}$, respectively [2]. The equation for the NLC elastic response is obtained by taking variations of this free energy. However, doing so results in a large system of equations [35]. To overcome this complexity, we note that in the examined configuration the molecular director and the electric field of the beam lie in the same (principal) plane (y, z); hence, as nonlinear reorientation occurs in this same plane and the azimuthal components can be neglected, the director $\vec{n}$ can be expressed in polar coordinates $\vec{n} = [0, \sin\psi, \cos\psi]$. Since the changes in molecular orientation along z are slow as compared with the wavelength of light, the derivatives with respect to z can also be neglected. In this approximation, the variations of the free energy (3) yield the Euler-Lagrange equation, where the subscripts on ψ denote derivatives,

$$\frac{\partial}{\partial x}\frac{\partial f}{\partial \psi_x} + \frac{\partial}{\partial y}\frac{\partial f}{\partial \psi_y} - \frac{\partial f}{\partial \psi} = 0, \tag{4}$$

leading to the director rotation in the form

$$\begin{aligned}
&K_{22}\frac{\partial^2\psi}{\partial x^2} + (K_{11}\cos^2\psi + K_{33}\sin^2\psi)\frac{\partial^2\psi}{\partial y^2} \\
&- \frac{1}{2}\sin 2\psi(K_{11} - K_{33})\left(\frac{\partial\psi}{\partial y}\right)^2 \\
&+ \frac{\varepsilon_0\Delta\varepsilon}{2}\left[2E_yE_z\cos 2\psi + \sin 2\psi(E_y^2 - E_z^2)\right] = 0.
\end{aligned} \tag{5}$$

Numerical solutions of this elliptic equation (5) are found using successive over-relaxations (SOR) with relaxation parameter $\Omega = 1.8$ [36]. When combined with the numerical solution of the electromagnetic model (1), solutions for beam propagation in nematic liquid crystals with varying orientation can be obtained. The director reorientation is recalculated after each 100 nm of propagation; after the first step in z, the solution for ψ is the initial guess for the SOR iterations, ensuring rapid convergence. The accuracy of the method described above can be estimated from the ratio of total input and output powers, which should be unity because absorption is neglected and the boundary conditions are purely reflective. Defining the relative error as $\eta = (P_{out} - P_{in})/P_{in}$, we aim to achieve $|\eta| < 0.5\%$ for all the cases considered here. In this work, the typical cell dimensions (thickness × width × length) are 30 μm × 200 μm × 500 μm and two simple anchoring conditions are analyzed, uniform and linearly varying, see Fig. 2. For the sake of a realistic analysis, we choose the material parameters corresponding to the common nematic liquid crystal 6CHBT, with Frank elastic constants

$K_{11} = 8.57$ pN, $K_{22} = 3.7$ pN and $K_{33} = 9.51$ pN and indices $n_\parallel = 1.6335$ and $n_\perp = 1.4967$ at temperature T=20°C and wavelength $\lambda = 2\pi/k_0 = 1.064\,\mu$m [15, 37]. The input beam is Gaussian and y-polarized, with a full width half maximum FWHM $= 7\,\mu$m and power 1 mW. Typical computer runs to obtain the results presented hereby in a single Intel Core i7 at 3.60 GHz took between 100 and 120 minutes for propagation lengths of 500 μm.

Momentum conservation

The full system (1) and (5) governing the propagation of a light beam in a non-uniform NLC cell is extensive and amenable to numerical solutions only. However, these equations can be simplified to yield a reduced system for which an adiabatic approximation applies based on the slow variation of the director orientation. This adiabatic approximation shows that the beam trajectory is determined by an overall "momentum conservation" (MC) equation. This is not physical momentum, but momentum in the sense of the invariances of the Lagrangian in the reduced system. Such reduction of the full system and the resulting momentum conservation equation will now be derived.

The first approximation is that the imposed linear modulation θ_b in the director orientation is much smaller than the constant background θ_0, $|\theta_b| \ll \theta_0$. For the examples considered here, typical values are $\theta_0 = 45°$ and maximum $|\theta_b|$ ranging from 5° to 20°. While the largest $|\theta_b|$ is not strictly much smaller than θ_0, nevertheless the asymptotic results are found to be in good agreement with the numerical ones even at this upper limit. As discussed in the previous section, we denote the additional nonlinear reorientation by θ, so that the total pointwise orientation is $\psi = \theta_0 + \theta_b + \theta$. In the paraxial, slowly varying envelope approximation, the equations (1) and (5) governing the propagation of the light beam through the NLC can be reduced to [2]

$$
\begin{aligned}
& ik_0 n_e \frac{\partial E_y}{\partial z} + 2ik_0 n_e \Delta(\psi) \frac{\partial E_y}{\partial y} + \nabla^2 E_y \\
& + k_0^2 \left(n_\perp^2 \cos^2\psi + n_\parallel^2 \sin^2\psi \right. \\
& \left. - n_\perp^2 \cos^2\theta_0 - n_\parallel^2 \sin^2\theta_0 \right) E_y = 0, \qquad \textbf{(6)}
\end{aligned}
$$

$$
K\nabla^2\psi + \frac{1}{4}\epsilon_0 \Delta\epsilon |E_y|^2 \sin 2\psi = 0. \qquad \textbf{(7)}
$$

As for the full equations of Section A, E_y is the complex valued envelope of the electric field of the beam, since in the paraxial approximation the components E_x and E_z are neglected. The Laplacian ∇^2 is in the transverse (x, y) plane. In the single constant approximation, the parameter K is a scalar on the assumption that bend, splay and twist in the full director equation (5) have comparable strengths. The wavenumber k_0 of the input light beam is intended in vacuum and n_e is the background extraordinary refractive index of the NLC [2]

$$
n_e^2(\psi) = \frac{n_\perp^2 n_\parallel^2}{n_\parallel^2 \cos^2\psi + n_\perp^2 \sin^2\psi}, \qquad \textbf{(8)}
$$

in the linear limit $\theta = 0$. The coefficient Δ is related to the birefringent walk-off angle δ of the extraordinary-wave beam, with $\tan\delta = \Delta$ in the (y, z) plane, and is given by

$$
\Delta(\psi) = \frac{\Delta\epsilon \sin 2\psi}{\Delta\epsilon + 2n_\perp^2 + \Delta\epsilon \cos 2\psi}. \qquad \textbf{(9)}
$$

Throughout this work, despite the nonlinear dependence of Δ on the beam power through the reorientation θ [38], we assume $\Delta = \Delta(\theta_0 + \theta_b)$ in the low power limit. In the single elastic constant approximation, the director equations (5) and (7) differ by a factor of $1/2$ in the dipole term involving $\epsilon_0\Delta\epsilon$, owing to definitions of the electric field based on either the maximum amplitude or the RMS (Root Mean Square) value. In this context, this difference is equivalent to a rescaling of K, with the latter constant K cancelling out in the adiabatic momentum conservation approximation.

The reduced equations (6) and (7) can be set in non-dimensional form via the variable and coordinate transformations

$$
x = WX, \quad y = WY, \quad z = BZ, \quad E_y = Au, \qquad \textbf{(10)}
$$

where

$$
\begin{aligned}
& W = \frac{\lambda}{\pi\sqrt{\Delta\epsilon \sin 2\theta_0}}, \quad B = \frac{2n_e\lambda}{\pi\Delta\epsilon \sin 2\theta_0}, \\
& A^2 = \frac{2P_0}{\pi\Gamma W^2}, \quad \Gamma = \frac{1}{2}\epsilon_0 c n_e \qquad \textbf{(11)}
\end{aligned}
$$

for a Gaussian input beam power of P_0 and wavelength λ [27]. With these non-dimensional variables, Eqs. (6) and (7) become

$$
\begin{aligned}
i\frac{\partial u}{\partial Z} + i\gamma\Delta(\theta_0 + \theta_b)\frac{\partial u}{\partial Y} + \frac{1}{2}\nabla^2 u & \\
+ 2\left(\theta_0 + \theta_b + \theta\right) u &= 0, \qquad \textbf{(12)} \\
\nu\nabla^2\theta &= -2|u|^2. \qquad \textbf{(13)}
\end{aligned}
$$

In deriving these equations we assumed that the NLC director rotation from θ_0 is small, i.e., $|\theta_b| \ll \theta_0$, as discussed above. We further assumed that the nonlinear response is small, with $|\theta| \ll \theta_0$. The trigonometric functions in the dimensional equations (6) and (7) have been expanded in Taylor series. The scaled parameters in these non-dimensional equations are

$$
\gamma = \frac{2n_e}{\sqrt{\Delta\epsilon \sin 2\theta_0}} \quad \text{and} \quad \nu = \frac{8K}{\epsilon_0\Delta\epsilon A^2 W^2 \sin 2\theta_0}. \qquad \textbf{(14)}
$$

The equations (12) and (13) have the Lagrangian formulation

$$
\begin{aligned}
L &= i\left(u^* u_Z - u u_Z^*\right) + i\gamma\Delta(\theta_0 + \theta_b)\left(u^* u_Y - u u_Y^*\right) \\
& - |\nabla u|^2 + 4\left(\theta_0 + \theta_b + \theta\right)|u|^2 - \nu|\nabla\theta|^2, \qquad \textbf{(15)}
\end{aligned}
$$

where the * superscript denotes the complex conjugate and the sub-indexes Z and Y denote derivatives. Equations (12) and (13) have no general exact solitary wave, or nematicon, solution; the only known exact solutions are for specific, related values of the parameters [39]. For this reason, variational and conservation law methods have proved to be useful to study nematicon evolution [39, 40], as they give solutions in good agreement with numerical and experimental results [27, 39, 40]. In particular, they provide accurate results for the refraction of nematicons due to variations in the dielectric constant [21, 41–43]. Conservation laws based on the Lagrangian (15) are used below to determine the nematicon trajectory in a cell with an imposed linear modulation of the orientation angle $\theta_0 + \theta_b$.

The easiest way to obtain the approximate momentum conservation equations for Eqs. (12) and (13) is from the Lagrangian (15) [28]. We assume the general functional forms

$$u = a g(\rho) e^{i\sigma + iV(Y-\xi)} \quad \text{and} \quad \theta = \alpha g^2(\mu), \tag{16}$$

where

$$\rho = \frac{\sqrt{X^2 + (Y-\xi)^2}}{w}, \quad \mu = \frac{\sqrt{X^2 + (Y-\xi)^2}}{\beta}, \tag{17}$$

for the nematicon and the director responses, respectively [28]. The actual beam profile g is not specified, as the trajectory is found to be independent of this functional form. In response to the change in the NLC refractive index, the extraordinary wave beam undergoes refraction, as well as amplitude and width oscillations. If the length scale of the refractive index change is larger than the beam width, the beam refraction decouples from the amplitude/width oscillations [21, 28, 42]. Consistent with this decoupling, the electric field amplitude a and the width w of the beam, the amplitude α and width β of the director response can be taken as constant if just the beam trajectory is required. Only the beam center position ξ and (transverse) "velocity" V are then taken to depend on Z, as well as the phase σ. This approximation is equivalent to momentum conservation for the Lagrangian (15) [44].

Substituting the profile forms (16) into the Lagrangian (15) and averaging by integrating in X and Y from $-\infty$ to ∞ [45] gives the averaged Lagrangian [40]

$$\begin{aligned}\mathcal{L}_m &= -2S_2\left(\sigma' - V\xi'\right)a^2w^2 - S_{22}a^2 \\ &\quad - S_2\left(V^2 + 2VF_1 - 4F\right)a^2w^2 + \frac{2A^2B^2\alpha\beta^2a^2w^2}{A^2\beta^2 + B^2w^2} \\ &\quad - 4\nu S_{42}\alpha^2 - 2qS_4\alpha^2\beta^2,\end{aligned} \tag{18}$$

where primes denote differentiation with respect to Z. Here F and F_1, which determine the beam trajectory, are expressed by

$$F(\xi) = \frac{\int_{-\infty}^{\infty}\int_{-\infty}^{\infty}(\theta_0 + \theta_b)\, g^2\, dXdY}{\int_{-\infty}^{\infty}\int_{-\infty}^{\infty} g^2\, dXdY}, \tag{19}$$

$$F_1(\xi) = \frac{\int_{-\infty}^{\infty}\int_{-\infty}^{\infty}\gamma\Delta\,(\theta_0 + \theta_b)\, g^2\, dXdY}{\int_{-\infty}^{\infty}\int_{-\infty}^{\infty} g^2\, dXdY}. \tag{20}$$

The integrals S_2, S_4 and S_{22} and S_{42} appearing in this averaged Lagrangian are

$$S_2 = \int_0^\infty \zeta g^2(\zeta)\, d\zeta, \quad S_{22} = \int_0^\infty \zeta g'^2(\zeta)\, d\zeta, \tag{21}$$

$$S_4 = \int_0^\infty \zeta g^4(\zeta)\, d\zeta, \quad S_{42} = \frac{1}{4}\int_0^\infty \zeta\left[\frac{d}{d\zeta}g^2(\zeta)\right]^2 d\zeta.$$

Taking variations of this averaged Lagrangian with respect to ξ and V yields the modulation equations

$$\frac{dV}{dZ} = 2\frac{dF}{d\xi} - V\frac{dF_1}{d\xi}, \tag{22}$$

$$\frac{d\xi}{dZ} = V + F_1, \tag{23}$$

which determine the beam trajectory. Eq. (22) is the momentum equation.

A simple reduction of the trajectory Eqs. (22) and (23) can be carried out when the beam width is much less than the length scale for the variation of the refractive index, that is the length scale of the variation of θ_b [28]. For the examples in this work, $\theta_b' \sim 0.002\,\text{rad}/\mu\text{m}$. Hence, a length scale for the variation of θ_b is 500 μm, while the typical beam width is 7 μm. The linear variation of the angle θ_b from the background angle θ_0 starts at $\theta_b = 0$ at $Y = 0$. Since the beam is launched at the mid-section of the cell $Y = L/2$, where the total angle in the absence of light is $\theta_0 + \theta_b(L/2) = \theta_m$, it is more accurate to expand the walk-off Δ in a Taylor series about θ_m rather than θ_0. If we set $\tilde{\theta}_b = \theta_b - \theta_b(L/2)$, the integrals F (19) and F_1 (20) can be approximated by

$$\begin{aligned}F(\xi) &\sim \theta_0 + \theta_b(\xi), \\ F_1(\xi) &\sim \gamma\Delta(\theta_0 + \theta_b(\xi)) \\ &= \gamma\Delta(\theta_m) + \gamma\Delta'(\theta_m)\tilde{\theta}_b(\xi) + \ldots\end{aligned} \tag{24}$$

We note that F_1 has been further approximated by expanding Δ in a Taylor series about θ_0 on taking $|\theta_b| \ll \theta_0$, discussed above. With this simplification, the trajectory equations (22) and (23) become

$$\frac{dV}{dZ} = \left(2 - V\gamma\Delta'(\theta_m)\right)\theta_b'(\xi), \tag{25}$$

$$\frac{d\xi}{dZ} = V + \gamma\Delta(\theta_m) + \gamma\Delta'(\theta_m)\tilde{\theta}_b(\xi). \tag{26}$$

The simplicity of the beam trajectory equations (25) and (26) enables exact solutions for simple angle modulations θ_b. The simplest is the linear case

$$\theta_b(Y) = \frac{\theta_r}{L}Y, \tag{27}$$

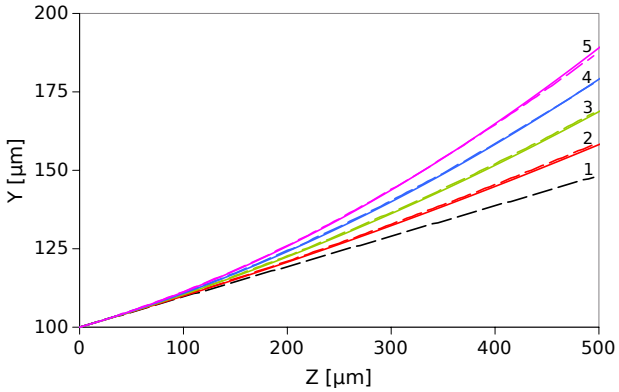

Fig. 3. (Color online) Numerical solutions of the NLC equations using FVBPM and elastic theory (dashed lines) and momentum conservation (28) (solid lines), describing nematicon evolution in a linearly modulated NLC anchoring in the cell. Red lines (labeled 2) $\theta_0 = 40^\circ$ to $\theta_r = 50^\circ$, green lines (labeled 3) $\theta_0 = 35^\circ$ to $\theta_r = 55^\circ$, blue lines (labeled 4) $\theta_0 = 30^\circ$ to $\theta_r = 60^\circ$ and violet lines (labeled 5) $\theta_0 = 25^\circ$ to $\theta_r = 65^\circ$. The black curve (labeled 1) refers to the uniform orientation case, with $\theta = 45^\circ$.

sketched in Fig. 2(b). For this linear case, θ_b goes from 0 at $Y = 0$ to θ_r at $Y = L$. This variation of θ_b enables the momentum equations (25) and (26) to be solved exactly and give the position of the beam center ξ as

$$\begin{aligned}\xi &= \left[\xi_0 + \frac{1+\gamma^2\Delta'(\theta_m)\Delta(\theta_m)}{\gamma^2\Delta'^2(\theta_m)\theta_b'}\right] e^{\gamma\Delta'(\theta_m)\theta_b' Z} \\ &\quad - \frac{2+\gamma^2\Delta'(\theta_m)\Delta(\theta_m)}{\gamma^2\Delta'^2(\theta_m)\theta_b'} \\ &\quad + \frac{1}{\gamma^2\Delta'^2(\theta_m)\theta_b'} e^{-\gamma\Delta'(\theta_m)\theta_b' Z} \end{aligned} \tag{28}$$

as $\tilde{\theta}_b' = \theta_b'$ is a constant. We assumed that the beam is launched at $\xi = \xi_0$ with $V = 0$ at $Z = 0$.

Since θ_b is slowly varying, the trajectory solution given by Eq. (28) can be expanded in a Taylor series to yield

$$\begin{aligned}\xi &\sim [\xi_0 + \gamma\Delta(\theta_m)Z] \\ &\quad + \left[\xi_0\left(\gamma\Delta'(\theta_m)\theta_b' Z + \frac{1}{2}\gamma^2\Delta'^2(\theta_m)\theta_b'^2 Z^2\right) + \right. \\ &\quad \left.\left(1 + \frac{1}{2}\gamma^2\Delta(\theta_m)\Delta'(\theta_m)\right)\theta_b' Z^2\right] + \ldots \end{aligned} \tag{29}$$

The first term in square brackets is the trajectory in a uniform NLC and the terms in the second set of square brackets are the correction due to a changing orientation. For the examples hereby, $\theta_b' \sim 0.002\ \text{rad}/\mu\text{m}$ and $\Delta' \sim 0.05/\mu\text{m}$. So, to first order in small quantities

$$\xi \sim [\xi_0 + \gamma\Delta(\theta_m)Z] + \theta_b' Z^2 \tag{30}$$

as $\Delta'(\theta_m)$ is small. Hence, the trajectory is described by the term for a uniform medium and a quadratic correction; the walk-off change due to the varying background director orientation dominates the change in the nematicon trajectory.

To convert the non-dimensional solution (28) back to dimensional variables, the scalings (11) are used. In particular, for the z scaling factor B, the angle for the extraordinary index (8) needs to be calculated. The obvious choice is to use the uniform background angle θ_0. However, while this leads to good agreement with the numerical solutions, near exact agreement is obtained by using the total director angle $\theta_0 + \theta_b$ in the absence of light. The imposed component θ_b is not constant, but a slowly varying (linear) function of Y, as discussed above, so its local value can be used to transform back to dimensional variables, consistent with a multiple scales analysis [46]. This local variation in the scaling factor for z gives a metric change in this coordinate, with a small, slowly varying alteration of the trajectory. Nevertheless, the overall effect of this small local change is significant over propagation distances of 500 μm and larger.

RESULTS AND DISCUSSION

Figure 3 shows a comparison of nematicon trajectories in the modulated NLC as given by the adiabatic momentum approximation (28) and by the FVBPM solution of the full system (1) and (5). The considered cell has a range of linear variations in the background director angle θ_b of the form (27). Each individual case, $\theta_0 + \theta_b$, is indicated in the figure. A Gaussian beam is launched at the center of the cell, with its trajectory becoming curved due to the non-uniform director alignment. In a uniform medium the (straight) nematicon trajectory is determined solely by the walk-off, which leads to a rectilinear path in the (y, z) plane. For the modulated uniaxial medium, not only the walk-off changes due to the varying anchoring, but the phasefront of the wavepacket is also distorted as the dielectric properties are modified and the NLC behaves like a lens with an index distribution n_e given by (8). Clearly, the momentum conservation approximation gives trajectories in close agreement with the numerical results. This validates the approximations made to arrive at the momentum conservation equations (25) and (26), in particular the assumption that the beam trajectory is not influenced by its amplitude-width oscillations. Furthermore, it shows how powerful such adiabatic approximations can be. Nonetheless, the momentum result is a kinematic approximation and so does not give all the information for the evolving beam, whereas the full system (1) and (5) can also provide the amplitude-width evolution. A final point regarding Figure 3 is that if the background angle for the extraordinary refractive index (8) in the z scaling (11) was chosen as θ_0 rather than $\theta_0 + \theta_b$, there would have been a noticeable difference between the momentum conservation and numerical results. The local variation of the propagation metric z due to the mod-

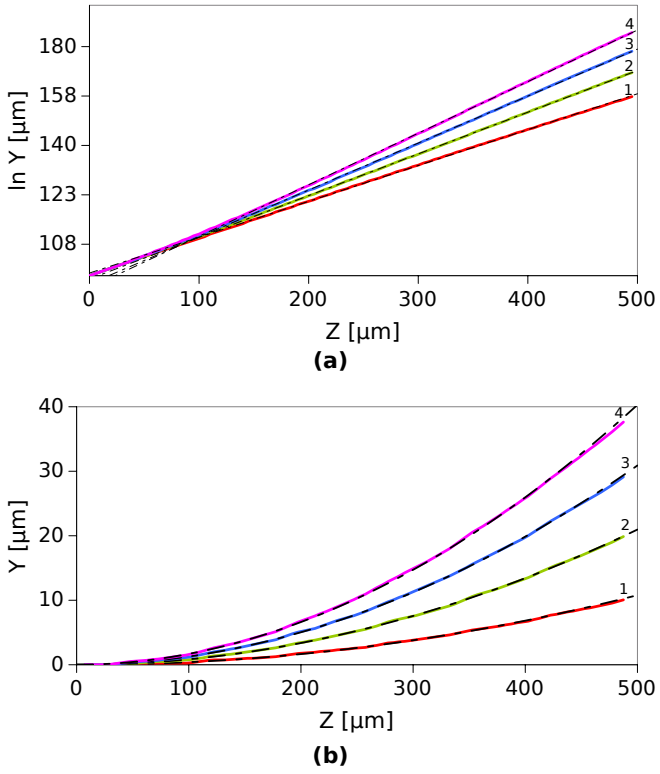

Fig. 4. FVBPM and elastic theory nematicon trajectory in a modulated cell: (a) logarithmic scale with exponential fitting and (b) linear scale after subtracting the trajectory in a uniform NLC ($\theta = 45°, \theta_b = 0$). Red line (labeled 1) $\theta_0 = 40°$ to $\theta_r = 50°$, green line (labeled 2) $\theta_0 = 35°$ to $\theta_r = 55°$, blue line (labeled 3) $\theta_0 = 30°$ to $\theta_r = 60°$ and violet line (labeled 4) $\theta_0 = 25°$ to $\theta_r = 65°$. Black dot-dashed line: (a) exponential fitting and (b) quadratic power fitting. Data fitted for $z > 100\,\mu$m.

ulated director angle in the absence of light, in fact, has a significant effect on beam propagation.

These results are further analyzed in Fig. 4(a). The data is plotted to a logarithmic scale with an exponential regression fitted through the numerical trajectories. As z increases the trajectories are well approximated by an exponential evolution, in agreement with the momentum conservation solution (28) as for large z the decaying exponential is negligible and the growing exponential dominates. Furthermore, when the rectilinear nematicon path in a uniform NLC is subtracted from the trajectory in the modulated case, the resulting beam position has a quadratic evolution in z, as shown in Fig. 4 (b). These exponential and quadratic fittings of the trajectories are consistent with θ_b' and Δ' being small, as demonstrated by reducing the full trajectory (28) to the quadratic approximation (30) via (29).

For a positive change of the anchoring conditions, i.e. $\theta_r > \theta_0$, walk-off and phase distortion both increase the beam deviation. In the opposite case for which $\theta_r < \theta_0$ these two phenomena counteract. The influence of walk-off and phase change on the nematicon path was analyzed for the case of the director orientation changing by $30°/200\,\mu$m, as shown in Fig. 5. When $\theta_r > \theta_0$ the beam bends strongly due to both the walk-off and phase distortions acting in the same direction, as illustrated in Fig. 5 (a). The phase change is strongest at the launch position as the molecules are oriented at approximately 45° there, so walk-off (given by (9) with $\psi = \theta_0 + \theta_b$) is close to its maximum. All the trajectories are monotonic and the beam transverse deviation increases with propagation distance. As for the comparisons in Figure 3, the agreement between the momentum conservation and numerical trajectories is near perfect, except for the lowest angle variation from 5° to 35°, for which the agreement is still satisfactory. In the latter case the initial director angle at the input is far from the walk-off maximum at 45°, so the trajectory bending is weak. Small errors in the momentum approximation then become relevant.

In the opposite case $\theta_0 > \theta_r$ the walk-off and the phase change along the cell counteract, resulting in the solitary beam reversing its transverse velocity, as illustrated in the comparison of Fig. 5 (b). The agreement between the momentum conservation and numerical trajectories is nearly perfect, except for two noticeable cases. The first is for the modulation from 35° to 5°, same interval but opposite sign than examined in the previous paragraph. The reason for the disagreement is again the weak bending of the beam and the enhanced role of small errors in the momentum approximation. The other case is the 75° to 45° modulation. It can be seen from Fig. 5 (b) that as the range of θ_b varies the beam reaches a maximum deviation in y. The 75° to 45° variation is just after this turning point. As for the 35° to 5° case, small errors in the momentum conservation approximation can then result in large trajectory deviations, in particular errors in the θ_b changes required for the maximum displacement in y.

Finally, we note that comparable beam powers are needed to obtain nematicons in uniform and linearly modulated NLCs, as a 1 mW input beam is sufficient to excite them in both cases, i.e. the rate of change in anchoring does not significantly modify the threshold power for reorientational solitons.

CONCLUSIONS

We have studied the propagation of reorientational optical spatial solitons in nematic liquid crystals encompassing a transversely modulated orientation of the optic axis (director). Even in the simplest limit of a linear change in anchoring angle, as considered here, non-uniform walk-off and wavefront distortion determine the bending of the resulting trajectory from the usual straight line, leading to curved paths and correspondingly curved optical waveguides induced by light beams through reorientation. Such modulations of the molecular director anchoring could be realized through electron-beam photolithography or

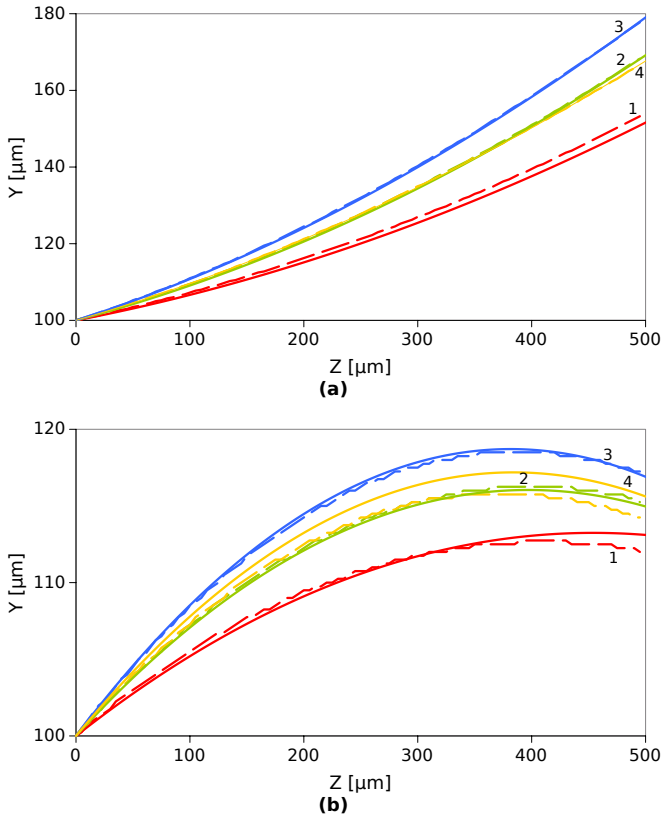

Fig. 5. Comparison of nematicon trajectories for (a) $\theta_r > \theta_0$ and (b) $\theta_r < \theta_0$. Numerical solutions of the nematic equations using FVBPM with elastic theory (dashed lines) and the momentum conservation (28) (solid lines). (a) Red lines (labeled 1) $\theta_0 = 5^\circ$ to $\theta_r = 35^\circ$; green lines (labeled 2) $\theta_0 = 15^\circ$ to $\theta_r = 45^\circ$; blue lines (labeled 3) $\theta_0 = 30^\circ$ to $\theta_r = 60^\circ$; yellow lines (labeled 4) $\theta_0 = 45^\circ$ to $\theta_r = 75^\circ$. (b) Red lines (labeled 1) $\theta_0 = 35^\circ$ to $\theta_r = 5^\circ$; green lines (labeled 2) $\theta_0 = 45^\circ$ to $\theta_r = 15^\circ$; blue lines (labeled 3) $\theta_0 = 60^\circ$ to $\theta_r = 30^\circ$; yellow lines (labeled 4) $\theta_0 = 75^\circ$ to $\theta_r = 45^\circ$. In all cases the rate of change is $30^\circ/200\,\mu$m.

photo-alignment techniques with light sensitive layers in order to define the boundary conditions in a point-wise manner. Experimental results have been recently reported in Ref. [47] using the former approach. Based on comparisons with numerical solutions obtained by FVBPM and elastic theory for self-localized light beam propagation in non-uniform nematic liquid crystals, we found that "momentum conservation" is an excellent approximation for modelling soliton paths in highly nonlocal media. It provides simple results for these trajectories and a highly intuitive explanation for their evolution, at variance with the highly coupled form of the full governing equations. While full numerical solutions can well describe nematicon evolution under generic conditions, the simplicity of the momentum conservation theory and its analytical solution speak in its favour for specific limits within the adiabatic category. Due to the slow variation of the anchoring conditions, both models show that the nematicon trajectory can be described as propagation in a uniform medium with a quadratic correction. Additionally, the power needed to excite reorientational solitons in either uniform or linearly non-uniform NLCs is comparable. Ongoing studies will address the role of longitudinal director modulations, as well as combinations of transverse and longitudinal changes, unveiling scenarios for the design of arbitrary soliton paths and corresponding all-optical waveguides. The latter results pave the way to novel generations of light-induced and light-controlled guided-wave circuits with two- and three-dimensional architectures.

ACKNOWLEDGEMENTS

F. A. Sala thanks the Faculty of Physics, Warsaw University of Technology, for a grant. U. A. L. thanks the National Centre for Research and Development in Poland under the grant agreement LIDER/018/309/L-5/13/NCBR/2014. G. Assanto thanks the Academy of Finland for support through the Finland Distinguished Professor grant no. 282858.

REFERENCES

1. G. I. Stegeman and M. Segev, "Optical spatial solitons and their interactions: Universality and diversity," *Science,* **286**, 1518–1523 (1999).
2. M. Peccianti and G. Assanto, "Nematicons," *Phys. Rep.*, **516**, 147–208 (2012).
3. I.-C. Khoo, *Liquid Crystals: Physical Properties and Nonlinear Optical Phenomena,* Wiley, New York (1995).
4. G. Assanto, A. Fratalocchi and M. Peccianti, "Spatial solitons in nematic liquid crystals: from bulk to discrete," *Opt. Express,* **15**, 5248–5259 (2007).
5. J.F. Henninot, M. Debailleul and M. Warenghem, "Tunable non-locality of thermal non-linearity in dye doped nematic liquid crystal," *Mol. Cryst. Liq. Cryst.,* **375**, 631–640 (2002).
6. J. Beeckman, K. Neyts, X. Hutsebaut, C. Cambournac and M. Haelterman, "Simulations and experiments on self-focusing conditions in nematic liquid-crystal planar cells," *Opt. Express,* **12**, 1011–1018 (2004).
7. A. Alberucci, A. Piccardi, M. Peccianti, M. Kaczmarek and G. Assanto, "Propagation of spatial optical solitons in a dielectric with adjustable nonlinearity," *Phys. Rev. A*, **82**, 023806 (2010).

8. A. Alberucci and G. Assanto, "Propagation of optical spatial solitons in finite-size media: interplay between nonlocality and boundary conditions," *J. Opt. Soc. Amer. B,* **24**, 2314–2320 (2007).
9. Y. V. Izdebskaya, V. G. Shvedov, A. S. Desyatnikov, W. Z. Krolikowski. M. Belic, Ga. Assanto and Y. S. Kivshar, "Counterpropagating nematicons in bias-free liquid crystals," *Opt. Express*, **18**, 3258–3263 (2010).
10. M. Kwasny, U.A. Laudyn, F.A. Sala, A. Alberucci, M.A. Karpierz and G. Assanto, "Self-guided beams in low-birefringence nematic liquid crystals," *Phys. Rev. A*, **86**, 013824 (2012).
11. M. Warenghem. J. Henninot and G. Abbate, "Non-linearly induced self waveguiding structure in dye doped nematic liquid crystals confined in capillaries," *Opt. Express*, **2**, 483–490 (1998).
12. M. Warenghem, J.F. Henninot and G. Abbate, "Bulk optical Freedericksz effect: non-linear optics of nematics liquid crystals in capillaries," *Mole. Crys. Liq. Cryst.,* **320**, 207–230 (1998).
13. M.A. Karpierz, "Solitary waves in liquid crystalline waveguides," *Phys. Rev. E,* **66**, 036603 (2002).
14. Y. Izdebskaya, V. Shvedov, G. Assanto and W. Krolikowski, "Magnetic routing of light-induced waveguides," *Nat. Comm.,* **8**, 14452 (2017).
15. M. Peccianti, A. Fratalocchi and G. Assanto, "Transverse dynamics of nematicons," *Opt. Express,* **12**, 6524-6529 (2004).
16. A. Piccardi, A. Alberucci, U. Bortolozzo, S. Residori and G. Assanto, "Readdressable interconnects with spatial soliton waveguides in liquid crystal light valves," *IEEE Photon. Techn. Lett.,* **22**, 694–696 (2010).
17. R. Barboza, A. Alberucci and G. Assanto, "Large electro-optic beam steering with nematicons," *Opt. Lett.,* **36**, 2725–2727 (2011).
18. A. Piccardi, A. Alberucci, R. Barboza, O. Buchnev, M. Kaczmarek and G. Assanto, "In-plane steering of nematicon waveguides across an electrically adjusted interface," *Appl. Phys. Lett.,* **100**, 251107 (2012).
19. F.A. Sala, M.A. Karpierz and G. Assanto, " Spatial routing with light-induced waveguides in uniaxial nematic liquid crystals," *J. Nonlin. Opt. Phys. Mater.,* **23**, 1450047 (2014).
20. M. Peccianti, A. Dyadyusha, M. Kaczmarek and G. Assanto, "Tunable refraction and reflection of self-confined light beams," *Nat. Phys.,* **2**, 737–742 (2006).
21. G. Assanto, A. A. Minzoni, N. F. Smyth and A. L. Worthy, "Refraction of nonlinear beams by localised refractive index changes in nematic liquid crystals," *Phys. Rev. A,* **82**, 053843 (2010).
22. Y. V. Izdebskaya, V. G. Shvedov, A. S. Desyatnikov, W. Krolikowski and Y. S. Kivshar, "Soliton bending and routing induced by interaction with curved surfaces in nematic liquid crystals," *Opt. Lett.,* **35**, 1692–1694 (2010).
23. A. Fratalocchi, A. Piccardi, M. Peccianti and G. Assanto, "Nonlinearly controlled angular momentum of soliton clusters," *Opt. Lett.,* **32**, 1447 (2007).
24. C. P. Jisha, A. Alberucci, R.-K. Lee and G. Assanto, "Optical solitons and wave-particle duality," *Opt. Lett.,* **36**, 1848–1850 (2011).
25. S. Slussarenko, A. Alberucci, C.P. Jisha, B. Piccirillo, E. Santamato, G. Assanto and L. Marrucci, "Guiding light via geometric phases," *Nat. Photon.,* **10**, 571–575 (2016).
26. A. Alberucci, C.P. Jisha, L. Marrucci and G. Assanto, "Electromagnetic waves in inhomogeneously anisotropic dielectrics: confinement through polarization evolution," *ACS Photon.,* **3**, 2249–2254 (2016).
27. G. Assanto, A. A. Minzoni, M. Peccianti and N. F. Smyth, "Optical solitary waves escaping a wide trapping potential in nematic liquid crystals: modulation theory," *Phys. Rev. A,* **79**, 033837 (2009).
28. B. D. Skuse and N. F. Smyth, "Interaction of two colour solitary waves in a liquid crystal in the nonlocal regime," *Phys. Rev. A,* **79**, 063806 (2009).
29. N.F. Smyth, A. Piccardi, A. Alberucci and G. Assanto, "Highly nonlocal optical response: Benefit or drawback?," *J. Nonlin. Opt. Phys. Mater.,* **25**, 1650043 (2016).
30. G. D. Ziogos and E. E. Kriezis, "Modeling light propagation in liquid crystal devices with a 3-D full-vector finite-element beam propagation method," *Opt. Quant. Electron.,* **40,** 733–748 (2008).
31. F. C. Frank, "I. Liquid crystals. On the theory of liquid crystals," *Discuss. Faraday Soc.,* **25**, 19–28 (1958).
32. C. W. Oseen, "The theory of liquid crystals," *Trans. Faraday Soc.,* **29**, 883–899 (1933).
33. F.A. Sala and M.A. Karpierz, "Modeling of nonlinear beam propagation in chiral nematic liquid crystals," *Mol. Cryst. Liq. Cryst.,* **558**, 176–183 (2012).
34. F.A. Sala and M.A. Karpierz, "Discrete diffractions and nematicons in chiral nematic liquid crystals," *Mol. Cryst. Liq. Cryst.,* **561**, 177–184 (2012).
35. F. Sala and M. A. Karpierz, "Modeling of molecular reorientation and beam propagation in chiral and non-chiral nematic liquid crystals," *Opt. Express,* **20**, 13923–13938 (2012).
36. L. Hageman and D. Young, *Applied Iterative Methods*, Academic Press, New York (1981).
37. M.J. Weber, *CRC Handbook of Laser Science and Technology: Optical Materials,* CRC Press, New York (1995).
38. M. Peccianti and G. Assanto, "Observation of power-dependent walk-off via modulational instability in nematic liquid crystals," *Opt. Lett.,* **30**, 2290–2292 (2005).
39. J. M. L. MacNeil, N. F. Smyth and G. Assanto, "Exact and approximate solutions for solitary waves in nematic liquid crystals," *Physica D,* **284**, 1–15 (2014).
40. A. A. Minzoni, N. F. Smyth and A. L. Worthy, "Modulation solutions for nematicon propagation in non-local liquid crystals," *J. Opt. Soc. Amer. B,* **24**, 1549–1556 (2007).
41. G. Assanto, N. F. Smyth and W. Xia, "Modulation analysis of nonlinear beam refraction at an interface in liquid crystals," *Phys. Rev. A,* **84**, 033818 (2011).
42. A. Alberucci, G. Assanto, A. A. Minzoni and N. F. Smyth, "Scattering of reorientational optical solitary waves at dielectric perturbations," *Phys. Rev. A,* **85**, 013804 (2012).
43. N. F. Smyth and W. Xia, "Refraction and instability of optical vortices at an interface in a liquid crystal," *J. Phys. B: Atomic, Molec. Opt. Phys.,* **45**, 165403 (2012).
44. D. J. Kaup and A. C. Newell, "Solitons as particles, oscillators, and in slowly changing media: a singular perturbation theory," *Proc. Roy. Soc. Lond. A,* **361**, 413–446 (1978).
45. G. B. Whitham, *Linear and Nonlinear Waves,* J. Wiley and Sons, New York (1974).
46. J. Kevorkian and J. D. Cole, *Perturbation Methods in Applied Mathematics,* Springer-Verlag, New York (1981).
47. U. Laudyn, M. Kwasny, F. Sala, M. Karpierz, N. F. Smyth and G. Assanto, "Curved solitons subject to transverse acceleration in reorientational soft matter," *Nature Sci. Rep.,* **7**, 12385 (2017).